Supplementary information to "Effects of the Electron Polarization on Dynamic Nuclear Polarization in Solids"

SI.1. Simulated and predicted populations during *d*CE DNP

In this SI we will show the steady state populations of the model spin system during MW irradiation. The black lines in Fig. SI.1 show the simulated populations, p_k^{sim}, with $D_{ab}/2\pi$ of (a) 0.8 MHz or (b) 20 MHz, using the parameters of table 1. The nuclear and electron polarizations in this system are plotted in Fig. 3 of the main article. The validity of the assumption expressed by eq. 5 was then tested by calculating the expected populations, p_k^{calc}, by deriving values of the η parameters from the simulated $P_{a/b/n}$ values using eq. 7, and inserting these values into eq. 6. These are plotted as dashed red lines in Fig. SI.1. Good agreement in the case of low dipolar interaction, for which eq. 5 was derived, and a lower agreement when this interaction is large, such that the MW irradiation saturates each of the electron SQ transitions to a different degree.

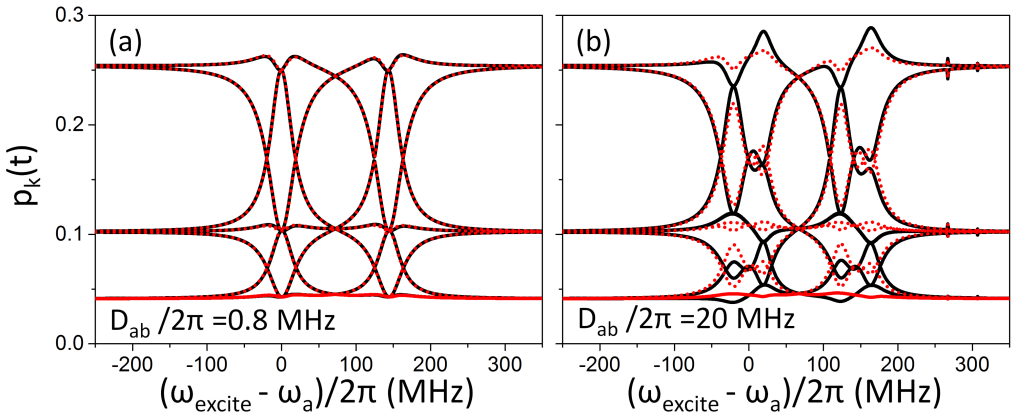

Figure SI.1: Simulated (black lines) and calculated (dashed red lines) populations in a model spin system. The parameters used in the simulation are given in Table 1. The calculation was performed based on the simulated electron and nuclear polarizations, as given in Fig. 3, using eqs. 6 and 7 in the main text.

SI.2. Multiple spin effects on the *i*CE mechanism

In this SI we show that multiple nuclear and electron couplings have a similar effect on the *i*CE mechanism as they do on the *d*CE mechanism[22, 54]. This can be seen in Fig. SI.2, where the polarization of the nucleus in a two electron, a and b, and one nucleus, n , $\{a-b-n\}$ system is plotted *versus* $(\omega_b-\omega_a-\omega_n)$ for several types of systems: (i) a four spins system with three electrons $\{c-a-b-n\}$ as already used in the main text; (ii) the same system as in (i) with the addition of a second nucleus, n_2, that is hyperfine coupled to e_b with $A_{z,bn_2}/2\pi$ =2 MHz (and neglecting the nuclear dipolar interaction); (iii) the same system as in (i) with the addition of an electron, d, dipolar coupled to e_a with a strength of $D_{ad}/2\pi = 1$ MHz; and (iv) a system with both a nucleus and an electron added. In all cases only the polarization of the original nucleus $P_n(t)$ is plotted. As can be seen, the addition of the second nucleus splits the CE condition, and results in a reduction of the maximal nuclear polarization. The same splitting occurs when the electron is added, but with only a small reduction of the polarization. The split transitions have different polarizations due to the low temperature used in the simulations. Finally, when both electron and nucleus added the polarization can almost be as high as for the isolated system. The significance of these effects are not yet clear when we are dealing with multi-spin systems.

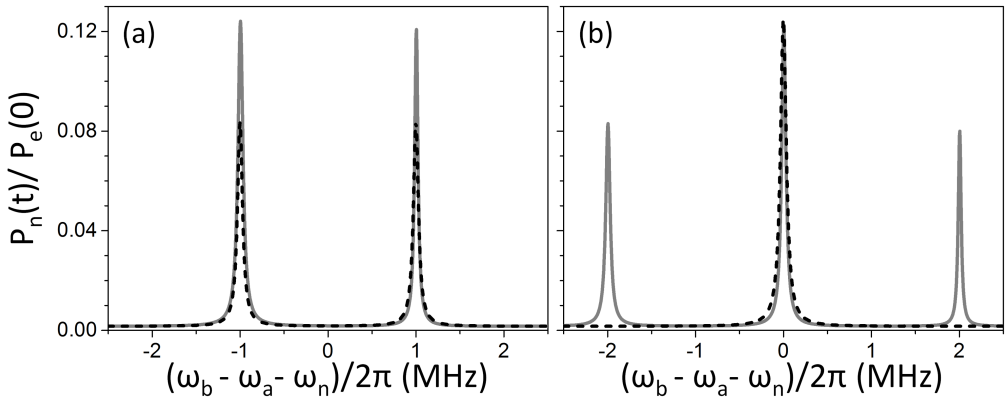

Figure SI.2: Multiple spin effects on the *i*CE mechanism. The simulated P_n nuclear polarization is plotted versus $(\omega_b-\omega_a-\omega_n)$ for a four spins system with three electrons $\{c-a-b-n\}$ as used in Fig. 2 (dashed black line in (b)); for the same system with an addition of a second nucleus, n_2, with $A_{z,bn_2}/2\pi = 2$ MHz and neglecting the nuclear dipolar interaction (dashed black line line in (a)); with the addition of an electron d, with $D_{ad}/2\pi = 1$ MHz (gray line in (a)); and a system with both the nucleus and the electron added (gray line in (b)). All other parameters are taken from Table 1.

SI.3. Signal processing of the ELDOR spectra

The acquired ELDOR spectra were processed as explained in section 5.1.1 in the main text. These were first obtained by collecting EPR signals as a function of the $\delta\nu_{excite}$ irradiation frequency, for a given detection frequency and temperature. These signals were subject to a baseline correction and integration over the position of the EPR echo. This resulted in a $E^{exp}_{excite}(\delta\nu_{excite})$ spectrum with arbitrary units. Next, the data was normalized with respect to of the "thermal" signal, S_0^{exp}, obtained by the average signal detected for MW irradiation far from any EPR transition. This resulted in the black line shown in Fig. SI.3, as measured using $\delta\nu_{detect} = -140$ MHz at 20 K. Since a part of the signal was given by a baseline which did not originate from the sample, a baseline correction S_b/S_0^{exp} was applied. These corrections are given by eq. 19 in the main text. In Fig. SI.3 an example of S_b/S_0^{exp}=0.1 (blue) or -0.1 (red) are shown, with the latter used in Fig. 6a in the main text.

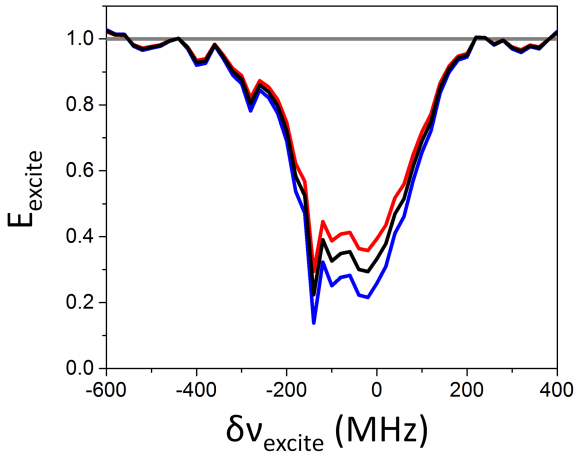

Figure SI.3: Signal processing of the ELDOR curves. This is shown here for the 40 mM sample TEMPOL described in the main article, with the ELDOR curves measured using $\delta\nu_{detect} = -140$ MHz at 20 K. The detected signals are rescaled using eq. 19 in the main text, such that the thermal signals (S_0^{exp}) are normalized to one (gray line) and a baseline artifact S_b is removed from the data. The effect of the latter is shown here using S_b/S_0^{exp} of 0 (black), 0.1 (blue), or -0.1 (red).